

Lennard-Jones triple-point bulk and shear viscosities. Green-Kubo theory, Hamiltonian mechanics, and nonequilibrium molecular dynamics

William G. Hoover

*Department of Applied Science, University of California at Davis/Livermore, Livermore, California 94550
and Lawrence Livermore National Laboratory, Livermore, California 94550*

Denis J. Evans

*Research School of Physical Sciences, Australian National University, Canberra, ACT 2600, Australia
and National Bureau of Standards, Boulder, Colorado 80303*

Richard B. Hickman

Lawrence Livermore National Laboratory, Livermore, California 94550

Anthony J. C. Ladd

Department of Applied Science, University of California at Davis/Livermore, Davis, California 95616

William T. Ashurst

Sandia Livermore Laboratory, Livermore, California 94550

Bill Moran

*Department of Applied Science, University of California at Davis/Livermore, Livermore, California 94550
and Lawrence Livermore National Laboratory, Livermore, California 94550*

(Received 24 March 1980)

A new Hamiltonian method for deformation simulations is related to the Green-Kubo fluctuation theory through perturbation theory and linear-response theory. Numerical results for the bulk and shear viscosity coefficients are compared to corresponding Green-Kubo calculations. Both viscosity coefficients depend similarly on frequency, in a way consistent with enhanced "long-time tails."

I. INTRODUCTION

Fluid flow can be treated at a variety of levels¹ by including only some of the difficulties associated with compressibility, viscosity, heat conduction, entropy production, gravity, and turbulence. In discussing shockwaves, only the last two of these complications can be ignored. The unique feature of shock compression² is the abrupt transformation of a fluid or solid from one equilibrium state to another. In a dense fluid this transformation can take place in approximately one atomic vibration time.³ The details of this irreversible transformation process depend upon the transient transport of momentum and energy within the shockwave front. With pressure jumps of tens of kilobars occurring in distances of only a few atomic diameters it is not clear *a priori* that a continuum point of view is appropriate to shockwaves at all. Nevertheless, it is known that the predicted shockwave profiles from the simplest reasonable continuum model—the Navier-Stokes equations, with compressibility, viscosity, conduction, and entropy production included—agree fairly well with profiles from atomistic computer simulations.^{3,4}

Viscosity is the physical property which domi-

nates shockwave structure. Viscosity describes the extra work required when deformation takes place rapidly, rather than slowly and reversibly. General deformations include both changes in shape and in size so that two different viscosity coefficients, shear (for shape) and bulk (for size) are required to describe the dependence of work on deformation rate.

In many flow problems changes in shape, involving only shear viscosity, are much more important than changes in size. In shockwave problems the bulk viscosity is equally important. Because the fluid density may change by a factor of two, the viscous irreversibility associated with rapid compression must be included. Because the only operational theory for bulk viscosity in dense fluids, the Enskog theory,⁵ is inadequate,⁶ we have undertaken a study of dense-fluid bulk viscosity. We have developed a new method for simulating fluid deformation, and here compare it with previous bulk-viscosity calculations. The new method can also be applied to shear flows, and has some interesting connections with the more usual Green-Kubo methods for calculating transport coefficients.

Green and Kubo showed that the transport coefficients describing nonequilibrium flows of mass,

momentum, and energy can be expressed in terms of the decay of equilibrium fluctuations of velocity, stress, and heat flux.⁷ Numerical decay calculations have been carried out for both hard⁸ and soft⁹ interparticle potential functions. Motivated both by the long times required for accurate equilibrium fluctuation calculations, and by the desire to develop an independent computational method as a check, several groups¹⁰⁻¹⁴ have carried out direct measurements of the transport coefficients using nonequilibrium molecular dynamics. In these direct approaches steady or oscillatory hydrodynamic states are maintained by performing external work. Phenomenological hydrodynamics is then used to relate the resulting mass, momentum, and energy fluxes to transport coefficients. The direct calculations are often more efficient than is the indirect approach of fluctuation theory, but suffer from the drawback that the results of the calculations must be extrapolated to the small-gradient limit of macroscopic hydrodynamics. The direct calculations make it possible to generate nonequilibrium distribution functions and to study nonlinear effects.

Shear flow and heat flow have both been simulated by carrying out molecular-dynamics calculations with "reservoirs" which maintain constant velocities and temperatures at the boundaries.^{12,15} The reservoirs themselves were kept at fixed velocities and temperature by external forces. Such forces do work on both the reservoirs' centers of mass and on the half-width of the reser-

voirs' velocity distributions relative to the center-of-mass velocities. These reservoir calculations provided estimates for the thermal conductivity and for the shear viscosity η which appears in Newton's phenomenological model¹⁶ for stress in a flowing fluid:

$$\bar{\sigma} = [\sigma_{0q} + \lambda \bar{\nabla} \cdot \bar{u}] \bar{I} + \eta [\bar{\nabla} \bar{u} + \bar{\nabla} \bar{u}^t]. \quad (1)$$

In (1) the stream velocity \bar{u} varies in space and time. The viscous contributions to the stress tensor $\bar{\sigma}$, over and above the equilibrium stress, are proportional to the symmetric tensors $\bar{\nabla} \cdot \bar{u} \bar{I}$, where \bar{I} is the unit tensor, and $\bar{\nabla} \bar{u} + \bar{\nabla} \bar{u}^t$, where t indicates transpose. The "second viscosity coefficient"¹⁷ λ can be expressed in terms of the bulk viscosity $\eta_v = \lambda + \frac{2}{3}\eta$.

The bulk viscosity describes the extra stress due to dilation in the absence of shear. Because this effect depends upon volume change—a change of thermodynamic state—bulk viscosity cannot be measured in a steady-state-reservoir experiment. If the volume is cycled over a small range, with a frequency ω , the constitutive relation (1) implies that in addition to the elastic stress, proportional to the strain and the adiabatic (frequency-dependent) bulk modulus B , there will also be a viscous stress proportional to the strain rate and the bulk viscosity. The bulk viscosity can be obtained either by determining the strain-rate component of stress, or by averaging the work done, by the forces cycling the volume, over a complete cycle of dilation and compression:

$$\int dW = \int \sigma dV = \int_0^{2\pi} d\omega t (3\xi V_0 \cos \omega t) (\sigma_{0q} + 3B\xi \sin \omega t + 3\eta_v \xi \omega \cos \omega t) = 9\pi \xi^2 V_0 \omega \eta_v. \quad (2)$$

In (2) ξ is the maximum one-dimensional strain amplitude. In a complete cycle, the elastic part of the stress does no work.

We have developed a method for simulating such a cyclic process by using nonequilibrium molecular dynamics.⁶ The viscosities resulting from such nonequilibrium simulations can be compared with Green-Kubo results and used to interpret the shockwave profiles from computer experiments.³ The new data should also stimulate improvements in two areas of dense-fluid transport theory—the data show that the Enskog theory of transport is inadequate for soft potentials and that the mode-coupling¹⁸ estimates of transport-coefficient frequency dependence are much too small¹⁴ near the triple point.

In the present work we first indicate the relation of our numerical method to the Green-Kubo theory. We then apply the method to a dense-fluid state

near the triple point. For this numerical work we have chosen to study the Lennard-Jones potential

$$\phi(r) = 4\epsilon [(\sigma/r)^{12} - (\sigma/r)^6], \quad (3)$$

at the same reduced density $N\sigma^3/V = 0.8442$, and reduced temperature $kT/\epsilon = 0.722$ studied by Levesque *et al.*⁹ Notice that in (3), in Sec. IV of the text, in the tables, and in the figures, σ and ϵ represent potential parameters rather than stress and strain.

II. HAMILTONIAN FOR ADIABATIC DEFORMATION

Any mechanical flow can be described by specifying the space and time dependence of the "strain-rate tensor" $\bar{\nabla} \bar{u}$. The tensor describes the rate at which any macroscopic coordinate q changes with time:

$$\dot{q} = \bar{q} \cdot \bar{\nabla} \bar{u}. \quad (4)$$

The two simplest such flows are homogeneous plane Couette flow (with du_x/dy the only nonzero element of $\vec{\nabla}\vec{u}$, for instance) and homogeneous dilation (with $\vec{\nabla}\vec{u}$ proportional to the unit tensor \vec{I}). If we consider a microscopic collection of N particles with coordinates \vec{q} (now, and in what follows, using \vec{q} to indicate a set of coordinates) and potential energy Φ , the application of the purely mechanical deformation (4) for a short time changes the potential energy: $\dot{\Phi} = -V\vec{P}_\phi : \vec{\nabla}\vec{u}$, where \vec{P}_ϕ is that part of the pressure tensor which depends upon the interparticle forces. In a thermodynamic deformation we expect to do work against the kinetic part \vec{P}_k , of the pressure too: $\dot{K} = -V\vec{P}_k : \vec{\nabla}\vec{u}$. This work is done exactly if we choose to vary the momenta in a way parallel to (4):

$$\dot{\vec{p}} = -\vec{\nabla}\vec{u} \cdot \vec{p}. \quad (5)$$

A microscopic Hamiltonian which incorporates not only the coordinate and momentum changes from (4) and (5), but also the usual changes from inertia and interparticle forces, is

$$\mathcal{H} = \Phi(\vec{q}) + K(\vec{p}) + \vec{q}\vec{p} : \vec{\nabla}\vec{u}. \quad (6)$$

The microscopic equations of motion derived from (6) are

$$\begin{aligned} \dot{\vec{q}} &= \partial\mathcal{H}/\partial\vec{p} = (\vec{p}/m) + \vec{q} \cdot \vec{\nabla}\vec{u}, \\ \dot{\vec{p}} &= -\partial\mathcal{H}/\partial\vec{q} = \vec{F} - \vec{\nabla}\vec{u} \cdot \vec{p}. \end{aligned} \quad (7)$$

The microscopic representation of the pressure tensor for a fluid with pairwise additive forces:

$$V\vec{P} = \vec{q}_i\vec{F}_{ij} + (\vec{p}\vec{p}/m), \quad (8)$$

can then be used to establish that the coupled equations of motion (7) satisfy exactly the first law of thermodynamics for adiabatic flow:

$$\dot{E} = -V\vec{P} : \vec{\nabla}\vec{u}, \quad (9)$$

where E is the internal energy $\Phi + (p^2/2m)$.

Thus the Hamiltonian (6) has the desirable feature of providing equations of motion consistent with thermodynamics. This Hamiltonian has other applications too. Anderson¹⁹ has just arrived independently at the same equations of motion (7). In his work, the pressure is treated as an independent variable to which the strain-rate responds. In our work the roles of pressure and strain-rate are reversed. Before proceeding to numerical applications of the equations of motion, we discuss the connection of the Hamiltonian and Green-Kubo fluctuation theory.

III. CONNECTIONS WITH GREEN-KUBO THEORY

There are two different ways to relate our perturbed Hamiltonian to conventional Green-Kubo theory. Let us consider first a treatment resembling

one of the several sketched by Zwanzig.⁷ For simplicity we choose a particular strain-rate tensor $\vec{\nabla}\vec{u} = \dot{\epsilon}\vec{I}$; this choice describes a homogeneous isotropic dilation. An analogous treatment applies for shear flows. Because the perturbed Hamiltonian describing this system includes a velocity gradient proportional to ϵ , we expect that in the limit of small strain rates $\dot{\epsilon} \rightarrow 0$, a thermodynamic system described by the Hamiltonian

$$\mathcal{H} = \Phi + K + \dot{\epsilon}\vec{q}\vec{p} : \vec{I}, \quad (10)$$

could also be correctly described by Newton's phenomenological model (1):

$$\begin{aligned} \langle PV \rangle_{\text{noneq}} &= \langle PV \rangle_{\text{eq}} - 3\dot{\epsilon}\eta_v V \\ &= \frac{1}{3} \langle \vec{q}_i\vec{p}_i \cdot \vec{F}_{ij} + (p^2/m) \rangle_{\text{noneq}}. \end{aligned} \quad (11)$$

If we introduce the Hamiltonian (10) into the ordinary canonical probability distribution

$$f_{\text{noneq}}/f_{\text{eq}} = \exp[-\dot{\epsilon}\vec{q}\vec{p} : \vec{I}/kT], \quad (12)$$

we find a simple expression for the bulk viscosity η_v :

$$-3\dot{\epsilon}\eta_v V = \frac{1}{3} \langle [-\dot{\epsilon}\vec{q} \cdot \vec{p}/kT][\vec{q}_i\vec{p}_i \cdot \vec{F}_{ij} + (p^2/m)] \rangle_{\text{eq}}. \quad (13)$$

The virial theorem⁵ can then be used to express the instantaneous pressure in (13) in terms of the dot product $\vec{q} \cdot \vec{p}$, giving

$$3PV = \vec{q}_i\vec{p}_i \cdot \vec{F}_{ij} + (p^2/m) = 3\bar{P}V + (d/dt)(\vec{q} \cdot \vec{p}), \quad (14)$$

where \bar{P} is the long-time-average pressure. Because the average value of $\vec{q} \cdot \vec{p}$ vanishes at equilibrium, (13) and (14) can be combined to give

$$\eta_v = \frac{1}{18} V kT \langle (d/dt)(\vec{q} \cdot \vec{p})^2 \rangle_{\text{eq}}. \quad (15)$$

This last relation can then be converted into the usual Green-Kubo autocorrelation form by writing the $\vec{q} \cdot \vec{p}$ as integrals of pressure fluctuations:

$$\begin{aligned} \eta_v &= \lim_{\tau \rightarrow \infty} \frac{V}{2\tau kT} \int_0^\tau ds \int_0^\tau dt \langle \delta P(s)\delta P(t) \rangle_{\text{eq}} \\ &= \frac{V}{kT} \int_0^\infty dt \langle \delta P(0)\delta P(t) \rangle_{\text{eq}}, \end{aligned} \quad (16)$$

where δP is $P - \bar{P}$. An essential step in this heuristic derivation is the smoothed, or coarse grained, evaluation of the time derivative in (15). The derivative approaches the value given by Newton's phenomenological model only at times exceeding microscopic relaxation times.

We next consider a more convincing derivation of (16) from (10), based on linear response theory.²⁰ This treatment resembles Kubo's calculation of the electrical conductivity.⁷ Linear response theory considers the effect of adding a perturbation $-A(\vec{q}, \vec{p})a(t)$ to the Hamiltonian, where A is a function of the coordinates and momenta and $a(t > 0)$ is a function of time. The theory expresses

the time behavior of the (arbitrary) response function R in terms of the correlation of dA/dt and R at different times:

$$\langle R(\vec{q}, \vec{p}) \rangle_{\text{noneq}} = \frac{1}{kT} \int_0^t ds a(s) \langle \dot{A}(0) R(t-s) \rangle_{\text{eq}}. \quad (17)$$

If we select for the response function the time derivative of the trace of Doll's tensor,

$$R \equiv \frac{d}{dt} (\vec{q} \cdot \vec{p}) = 3PV(t) - 3\bar{P}V(t), \quad (18)$$

where the long-time-average pressure $\bar{P} [= \bar{P}(0) - 3B^s\epsilon(t)]$ is evaluated at the volume $V(t)$ and internal energy $E(t)$,²¹ and if we use the phenomenological viscoelastic equation of state,^{22,23} valid for small strains and strain rates, we have

$$\begin{aligned} \langle R(t) \rangle_{\text{noneq}} &= 9[B^s - B(\omega)]V\dot{\epsilon}(t) - 9\eta_v(\omega)V\dot{\epsilon}(t) \\ &= -\frac{V^2}{kT} \int_0^t ds 9\dot{\epsilon}(t-s) \langle \delta P(0)\delta P(s) \rangle_{\text{eq}}, \quad (19) \end{aligned}$$

where ϵ is the strain, $\epsilon = \xi \sin\omega t$, and $\delta P = P - \bar{P}$. The short-time limit of (19) reproduces Zwanzig and Mountain's relation²³ between the infinite-frequency bulk modulus and equilibrium pressure fluctuations. For long times the upper limit in the integral can be replaced by infinity; (19) can then be separated into two independent equations, one for $\sin\omega t$ and one for $\cos\omega t$. These establish the well-known results for the frequency-dependent bulk modulus $B(\omega)$ and bulk viscosity $\eta_v(\omega)$:

$$B(\omega) - B^s = \frac{V}{kT} \int_0^\infty d\omega t \sin\omega t \langle \delta P(0)\delta P(t) \rangle_{\text{eq}}, \quad (20)$$

$$\eta_v(\omega) = \frac{V}{kT} \int_0^\infty dt \cos\omega t \langle \delta P(0)\delta P(t) \rangle_{\text{eq}}. \quad (21)$$

Thus we obtain the Newtonian liquid model from the microscopic equations as a direct long-time limit of linear-response theory. In the case that

$\vec{\nabla} \cdot \vec{u}$ is chosen to correspond to a shear flow, a similar calculation provides the Green-Kubo formulas for the shear modulus $G(\omega)$ and the shear viscosity $\eta(\omega)$. Although the bulk and shear relations are "well-known," the methods used here to derive them are remarkably direct. In the next section we consider numerical applications of the Hamiltonian for adiabatic deformation.

IV. LENNARD-JONES TRIPLE-POINT CALCULATIONS

The Lennard-Jones thermodynamic state $N\sigma^3/V = 0.8442$, $kT/\epsilon = 0.722$ has been studied exhaustively.^{9,12} This state corresponds to liquid argon near the triple point if σ and ϵ/k are given the values 3.405 Å and 119.8 K. The published Green-Kubo shear viscosity⁹ has recently been supplemented by unpublished calculations carried out by Levesque in France and Pollock in America. We have also extended the earlier steady homogeneous-shear calculations,¹² which treated successively wider systems of 108, 2×108 , and 3×108 particles, by carrying out a calculation with a width eight times that of a 108-particle cube. These results are all summarized in Table I. The unpublished results of Levesque and Pollock for 108 to 500 particles agree fairly well with each other and with the experimental shear viscosity for liquid argon, expressed in terms of the atomic mass m , σ , and ϵ . The French 864-particle data, both published and unpublished, deviate from the rest. The directly calculated reservoir calculations are also summarized in the table, and agree with all but the 864-particle results. The two homogeneous-shear calculations for the shear viscosity use slightly different (steady *versus* oscillatory) algorithms—Denis Evans will publish details of his calculations (Table II) separately.

We have verified that the present perturbed-Hamiltonian method reproduces correctly the

TABLE I. Green-Kubo, reservoir, and homogeneous-shear values for the Lennard-Jones shear viscosity in the vicinity of the triple point. These calculations were carried out at a reduced density $N\sigma^3/V$ of 0.8442 and typically include 10^5 time steps.

N	kT/ϵ	$\eta\sigma^2/(m\epsilon)^{1/2}$	Type	Source
108	0.728	2.97	GK	Levesque
256	0.715	2.92	GK	Levesque
256	0.722	2.6 ± 0.1	GK	Pollock
500	0.722	3.2 ± 0.2	GK	Pollock
864	0.722	3.85	GK	Levesque
864	0.722	4.03	GK	Ref. 9
108-324	0.722	2.95 ± 0.2	R, H	Ref. 12
108 × 8	0.715	3.0 ± 0.15	H	Present work (steady shear)
108	0.722	3.18 ± 0.1	H	(Table II) (oscillatory)
Experimental estimate:		3.0		Ref. 25

TABLE II. Lennard-Jones shear viscosity near the triple point obtained by applying homogeneous oscillatory isothermal shear. These results were all obtained with Lennard-Jones's potential truncated at 2.5σ and with a timestep of $0.007\sigma(m/\epsilon)^{1/2}$; $N=108$, $N\sigma^3/V=0.8442$, and $\hbar T/\epsilon=0.722$. Amplitude times frequency $\xi\omega$, frequency ω , and number of shearing cycles are listed.

$\xi\omega\sigma(m/\epsilon)^{1/2}$	$\omega\sigma(m/\epsilon)^{1/2}$	$\eta\sigma^2/(m\epsilon)^{1/2}$	Cycles
0	0 ^a	3.18±0.1	
0.10	8.98	1.27	770
0.20	1.12	2.70	25
0.20	2.24	2.18	100
0.20	4.49	1.74	100
0.20	8.98	1.22	200
0.20	11.98	1.10	533
0.20	14.96	0.90	333
0.30	1.12	2.41	32
0.30	2.24	2.33	80
0.30	4.49	1.72	100
0.30	8.98	1.25	200
0.30	11.97	1.14	267

^a Extrapolation from Ref. 14.

shear viscosities already obtained using external reservoirs. To enhance the importance of the kinetic contribution to the shear flow (almost negligible at the triple point) we carried out a shear-flow simulation at a reduced density of 0.45 with a reduced temperature of 2.16. Both this perturbed-Hamiltonian calculation and the external-reservoir calculation give 108-particle viscosities of $(0.45 \pm 0.02)(m\epsilon)^{1/2}/\sigma^2$, with nearly equal contributions from the kinetic and potential parts of the momentum flux. A trial calculation was carried out to assess the importance of the perturbation force $F_y = -(du_x/dy)p_x$; when this essential term was omitted the kinetic contribution to the shear viscosity was reduced from $0.23(m\epsilon)^{1/2}/\sigma^2$ to nearly zero.

For bulk viscosity the only previous calculations used the Green-Kubo method—there is no bulk-viscosity analog for the reservoir calculations

used to simulate shear flow. The Green-Kubo results are summarized in Table III. Again we have included recent unpublished calculations carried out by Levesque. We have carried out a series of lengthy calculations using the equations of motion

$$\dot{\vec{q}} = (\vec{p}/m) + \dot{\epsilon}\vec{q}, \quad \dot{\vec{p}} = \vec{F} - \dot{\epsilon}\vec{p}. \quad (7')$$

It is convenient to solve these first-order equations using a standard packaged routine.²⁴ We also add to the set of $6N$ equations the adiabatic equation for conservation of energy:

$$\dot{E} = -3\dot{\epsilon}VP. \quad (9')$$

The integrated energy change over a cycle of dilation and compression can then be compared with the change in the internal energy over the cycle, calculated from $\Phi + K$ with the initial and the final coordinates and momenta. We chose a timestep such that these two independent estimates of the hysteresis agreed to about one part in ten thousand. At the end of every compressional cycle the particle momenta p were rescaled so that the next cycle would begin with the desired initial internal energy. After completing most of the calculations we found that the computation could be made considerably faster by adding a small term, proportional to r^{*6} , to the pair potential to make the forces vanish continuously at the potential cutoff.

Each calculation began in a body-centered-cubic initial state with a Maxwell-Boltzmann velocity distribution chosen to give the same thermal (i.e., relative to a perfect crystal) energy per particle as that found for 864 particles by Levesque *et al.*⁹ Melting was enhanced by the bcc structure and a check of the temperature indicated that there was no difficulty in melting to form a liquid state. Although only the first cycle appeared obviously anomalous we took the precaution of discarding the first ten cycles.

The adiabatic external work for each cycle can be separated into potential and kinetic components, but these have no particularly simple significance

TABLE III. Comparison of Green-Kubo bulk viscosities for the Lennard-Jones potential with the present calculations. The densities and temperatures for Levesque's unpublished calculations correspond to those given in Table I.

N	$\eta_b\sigma^2/(m\epsilon)^{1/2}$	Type	Source
108	1.13	GK	Levesque
256	0.89	GK	Levesque
864	1.04	GK	Levesque
864	1.05	GK	Ref. 9
54	1.55		Present work
Experimental estimate:	2.0		Ref. 25

for the Lennard-Jones potential. It is interesting to point out that for the simpler inverse-power potentials, the virial-theorem relation between the pressure and the energy,

$$3PV = 2K + n\Phi, \quad (22)$$

allows us to calculate separately the strain-rate dependence of the potential and kinetic energies and to relate these two terms to the strain-rate dependence of the pressure, which is still given by (22). In general the potential contribution to the bulk viscosity is $-\frac{1}{2}n$ times the kinetic contribution for an inverse- n th-power pair potential.

The link between the potential and kinetic parts of the (constant-energy) pressure fluctuations leads to interesting conclusions. For the inverse- n th-power potential, the ratio of the "potential" to "cross" to "kinetic" terms in the Green-Kubo bulk viscosity integrand is *exactly* $\frac{1}{2}n^2$ to $-n$ to 1.

For a general force law, linear-response theory, applied to the many-body Hamiltonian (10), can be used to show directly that *exactly* half the cross term contributes to the kinetic part of the bulk (or shear) viscosity; the remaining half contributes to the potential part. Thus, in the inverse-12th-power "soft-sphere" case, the potential "long-time tail" for bulk viscosity is 36 times larger than the kinetic one. The simple relationships between the potential and kinetic parts of the pressure fluctuations have been verified numerically for the inverse-12th-power soft-sphere potential in a series of bulk-viscosity calculations.⁶ A numerical analysis for the Lennard-Jones potential should be carried out.

The numerical results of our Lennard-Jones triple-point calculations are given in Table IV

TABLE IV. Perturbed-Hamiltonian bulk viscosity for the nearest-image Lennard-Jones potential at $N\sigma^3/V = 0.8442$ and $kT/\epsilon = 0.722$. The amplitude ξ , frequency ω , and number of dilation-compression cycles are listed.

N	ξ	$\omega\sigma(m/\epsilon)^{1/2}$	$\eta_b\sigma^2/(m\epsilon)^{1/2}$	Cycles
54	0.02	1	1.10 ± 0.06	800
54	0.02	2	0.82 ± 0.04	500
54	0.02	3	0.71 ± 0.02	1000
54	0.02	4	0.61 ± 0.02	1000
54	0.02	5	0.52 ± 0.02	200
54	0.02	6	0.51 ± 0.01	1000
54	0.02	7	0.50 ± 0.02	500
54	0.02	8	0.45 ± 0.02	500
54	0.02	9	0.48 ± 0.02	500
54	0.02	10	0.45 ± 0.02	200
54	0.01	10	0.48 ± 0.03	1000
128	0.02	10	0.45 ± 0.02	200
250	0.02	10	0.45 ± 0.01	200

(see also Fig. 1). Each calculation depends upon three separate parameters; the number of particles N , the strain amplitude ξ , and the frequency ω . The data show that the number dependence is small, at least at high frequency. The dependence on strain amplitude is harder to assess. Small amplitudes give large fluctuations in the hysteresis per cycle, while large strain amplitudes include a wider range of densities. For the most part our calculations were limited to a single maximum amplitude $\xi = 0.02$.

The bulk and shear viscosities vary similarly with frequency. The homogeneous-shear data (see Fig. 1) were calculated with both the temperature and the frequency held constant. These shear-viscosity results, for the range of frequencies and strain rates corresponding to our own bulk-viscosity calculations, can be described by the empirical relation

$$\eta\sigma^2/(m\epsilon)^{1/2} \sim 3.18 - 0.65(m/\epsilon)^{1/4}(\sigma\omega)^{1/2}. \quad (23)$$

If this dependence *actually* holds in the MHz to GHz range of laboratory experiments, it should be

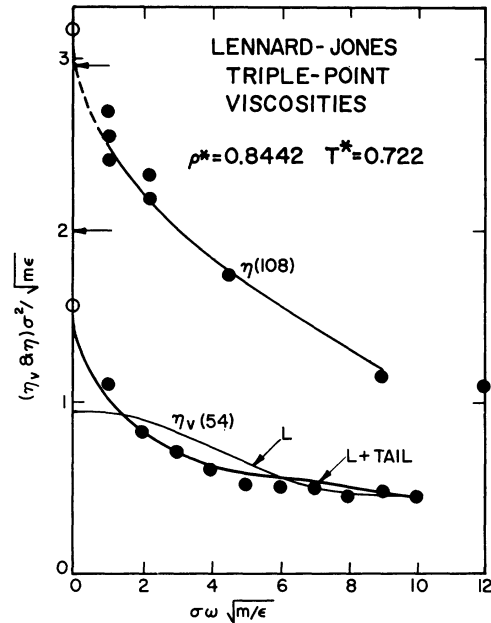


FIG. 1. Computer-generated homogeneous-shear isothermal shear viscosities and perturbed-Hamiltonian bulk viscosities are shown as filled circles. Experimental estimates of the low-frequency viscosities for liquid argon are indicated by the horizontal arrows. The phenomenological fit (23) is shown for the shear viscosity. In the bulk-viscosity case the L line gives the frequency-dependent viscosity from a numerical integration of Levesque's data as shown in Fig. 2. The L +tail line indicates the effect of an enhanced long-time tail corresponding to Eq. (24) of the text. The intercepts for both the shear and bulk fits are shown as open circles.

possible to observe noticeable frequency-dependent effects.

The bulk-viscosity results have a form similar to the shear data. If we use the same square-root dependence of viscosity on frequency, the extrapolated hydrodynamic bulk viscosity lies close to current experimental estimates.²⁵ At the same time, this extrapolation

$$\eta_v \sigma^2 / (m\epsilon)^{1/2} \sim 1.55 - 0.55(m/\epsilon)^{1/4}(\sigma\omega)^{1/2}, \quad (24)$$

lies considerably above the Green-Kubo (zero-frequency) estimates. It is difficult to settle the question of the long-time or low-frequency dependence of the viscosities by numerical calculation. Levesque's and Pollock's Green-Kubo data indicate considerable number dependence at long times and our own results cannot be pushed to lower frequencies without substantial improvements in the efficiency of numerical simulations.

Nevertheless, a self-consistent picture of the long-time and low-frequency behavior does emerge if we combine Levesque's bulk-viscosity integrand—his data are shown for 108 and 864 particles in Fig. 2—with the long-time tail consistent with the low-frequency relation (24). The coefficient required, $0.55/(2\pi)^{1/2} = 0.22$ in the units of Fig. 2, is only slightly less than the $0.65/(2\pi)^{1/2} = 0.26$ required by Evans's shear-viscosity data.

The result of adding the tail correction to the Green-Kubo data is shown in Fig. 1. The tail changes the overall curvature of the plot from negative to positive and brings about excellent agreement between the equilibrium and nonequilibrium data. The calculated bulk viscosity, 1.55 in the units of Fig. 1, is not too far below the ex-

perimental estimate²⁵ for liquid argon 2.0. The good agreement linking the Green-Kubo correlation function to our nonequilibrium simulations and to experiment is gratifying. It suggests that the present methods can be used with confidence for other thermodynamic states and for other force laws.

The shear-viscosity results are less consistent. Integration of the large-system ($N = 864$) Green-Kubo integrand, with or without an appended long-time tail, gives viscosities substantially higher than either the small-system or experimental estimates.

V. DISCUSSION

The perturbed-Hamiltonian approach to nonequilibrium deformation is aesthetically pleasing because it is so closely related to thermodynamics and equilibrium fluctuation theory. This same Hamiltonian should prove to be useful in attempts to understand theoretically the frequency and amplitude dependence of the viscosities.

It would be useful to find an analogous formulation for diffusion and heat conduction, but our attempts to do this for conduction have failed. It is easy to use an extra force proportional to each particle's energy fluctuation to drive a homogeneous isothermal heat current with nonequilibrium molecular dynamics. It is not so easy to find a simple isochoric (as opposed to adiabatic) analog of the first law of thermodynamics. Nevertheless, we expect that the heat current resulting from the perturbation just described, will provide a perfectly useful approach to thermal conductivity. We expect to carry out such calculations for comparison with the earlier reservoir and Green-Kubo work.^{9,15}

The present bulk-viscosity results show once again⁶ that the Enskog theory is a poor approximation for potentials as soft as r^{-12} . The hard-sphere prediction, underlying that theory, that the frequency changes in the bulk and shear moduli are similar at high density fails for soft potentials. For soft forces the high- and low-frequency bulk moduli are similar, so that the bulk viscosity is relatively small. The present data underscore the need for theoretical understanding of dense-fluid transport. In particular, the mode-coupling predictions,¹⁸ even if they turn out to be correct for frequencies below those which can be studied in computer simulations, are grossly in error for the frequencies studied here. Because even a relatively crude theory would be welcome, it seems possible that models based on cell theories incorporating perturbed equations of motion will turn out to be useful.

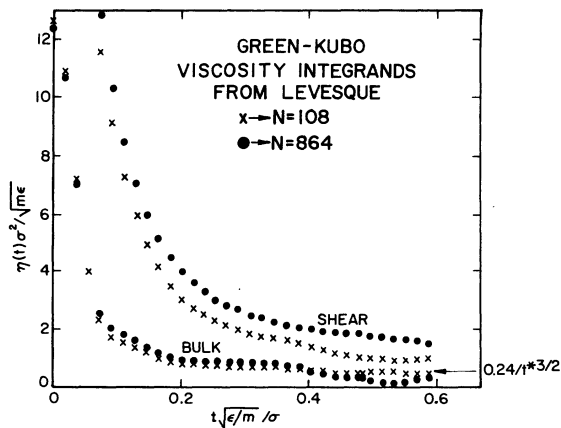


FIG. 2. Equilibrium fluctuation correlation functions calculated by Levesque. The nonequilibrium calculations described in the text suggest a long-time tail at about the level indicated by the arrow (0.26 for shear, 0.22 for bulk).

Notes added in proof. (i) The Doll's-tensor Hamiltonian can also be used to obtain equilibrium fluctuation expressions for nonequilibrium distribution functions. See D. J. Evans, W. G. Hoover, and A. J. C. Ladd, *Phys. Rev. Lett.* **45**, 124 (1980). (ii) Bill Wood and Bob Dorfman kindly pointed out to us that in Ernst, Hauge, and van Leeuwen's work [*J. Stat. Phys.* **15**, 7 (1975)], the kinetic part of the pressure fluctuation is *defined* to be zero. We alert the reader that this peculiar choice is different from ours, as described following Eq. (22).

ACKNOWLEDGMENTS

Gary Doolan made useful suggestions for implementing a vectorized version of our calculations on the CRAY computer. We thank Roy Pollock

for carrying out the two shear-viscosity Green-Kubo calculations in Table I. We are particularly grateful to Dr. Levesque for making his unpublished data available. In view of the confusion surrounding Fig. 2 of Ref. 9, the new data were indispensable in correlating the equilibrium and nonequilibrium viscosities. This work was performed under the auspices of the U.S. Department of Energy at the Lawrence Livermore National Laboratory under contract No. W-7405-ENG and supported, in part, at UC Davis, by the Army Research Office, Research Triangle Park, North Carolina. Partial accounts of this work were presented by W. G. Hoover at the M. S. Green Statistical Physics Symposium, 24-25 April 1980, Gaithersburg, Maryland and at the Sitges (Spain) Symposium, 9-13 June 1980.

-
- ¹B. Lé Mehauté, *An Introduction to Hydrodynamics and Water Waves* (Springer, Berlin, 1976).
- ²Y. B. Zeldovich and Y. P. Raizer, *Physics of Shock Waves and High-Temperature Hydrodynamic Phenomena* (Academic, New York, 1967).
- ³V. Y. Klimenko and A. N. Dremin, in *Detonatsiya, Chernogolovka*, edited by O. N. Breusov *et al.* (Akad. Nauk, Moscow, SSSR, 1978), p. 79; B. L. Holian, W. G. Hoover, B. Moran, and G. K. Straub, *Phys. Rev. A* (to be published).
- ⁴W. G. Hoover, *Phys. Rev. Lett.* **42**, 1531 (1979).
- ⁵J. O. Hirschfelder, C. F. Curtiss, and R. B. Bird, *Molecular Theory of Gases and Liquids* (Wiley, New York, 1954).
- ⁶W. G. Hoover, A. J. C. Ladd, R. B. Hickman, and B. L. Holian, *Phys. Rev. A* **21**, 1756 (1980); W. G. Hoover and R. B. Hickman, *Bull. Am. Phys. Soc.* **25**, 550 (1980).
- ⁷R. W. Zwanzig, *Ann. Rev. Phys. Chem.* **16**, 67 (1965).
- ⁸B. J. Alder, D. M. Gass, and T. E. Wainwright, *J. Chem. Phys.* **53**, 3813 (1970).
- ⁹D. Levesque, L. Verlet, and J. Kürkijarvi, *Phys. Rev. A* **7**, 1690 (1973). Note that the "bulk"-viscosity integrand in Fig. 2 of LVK is actually the *shear*-viscosity integrand and that the quoted thermal conductivity is in error by about a factor of two. (D. Levesque, private communications.)
- ¹⁰E. M. Gosling, I. R. McDonald, and K. Singer, *Mol. Phys.* **26**, 1475 (1973).
- ¹¹A. W. Lees and S. F. Edwards, *J. Phys. C* **5**, 1921 (1972).
- ¹²W. T. Ashurst and W. G. Hoover, *Phys. Rev. A* **11**, 658 (1975).
- ¹³T. Naitoh and S. Ono, *J. Chem. Phys.* **70**, 4515 (1979).
- ¹⁴D. J. Evans, *Phys. Lett.* **74A**, 229 (1979) and *J. Stat. Phys.* **22**, 81 (1980).
- ¹⁵W. G. Hoover and W. T. Ashurst, in *Theoretical Chemistry, Advances and Perspectives*, edited by H. Eyring and D. Henderson (Academic, New York, 1975), Vol. 1, p. 1.
- ¹⁶S. G. Brush, *Kinetic Theory* (Pergamon, New York, 1972), Vol. 3.
- ¹⁷L. Rosenhead, *Proc. R. Soc. London Ser. A* **226**, 1 (1954).
- ¹⁸Y. Pomeau and P. Résibois, *Phys. Rep.* **19**, 63 (1975).
- ¹⁹H. C. Andersen, *J. Chem. Phys.* **72**, 2384 (1980).
- ²⁰D. A. McQuarrie, *Statistical Mechanics* (Harper and Row, New York, 1976), p. 507.
- ²¹J. A. McLennan, *Prog. Theor. Phys. Jpn.* **30**, 408 (1963).
- ²²J. Frenkel, *Kinetic Theory of Liquids* (Dover, New York, 1955).
- ²³R. W. Zwanzig and R. D. Mountain, *J. Chem. Phys.* **43**, 4464 (1965).
- ²⁴L. F. Shampine and M. K. Gordon, *Computer Solution of Ordinary Differential Equations* (Freeman, San Francisco, 1975).
- ²⁵S. A. Mikhailenko, B. G. Dudar, and V. A. Schmidt, *Fiz. Nizk. Temp.* **1**, 224 (1975) [*Sov. J. Low Temp. Phys.* **1**, 109 (1975)].